Sensors & Actuators: B. Chemical 310 (2020) 127890

Contents lists available at ScienceDirect

Sensors and Actuators B: Chemical

journal homepage: www.elsevier.com/locate/snb

Two quenching groups are better than one: A robust strategy for constructing HOCl fluorescent probe with minimized background fluorescence and ultra-high sensitivity and its application of HOCl imaging in living cells and tissues

Guansheng Zheng[a,b,1], Zejun Li[a,1], Qinya Duan[a,1], Ke Cheng[b,c], Yong He[a], Shumei Huang[a], Huatang Zhang[a,*], Yin Jiang[a,*], Yongguang Jia[d], Hongyan Sun[b,c,**]

[a] School of Chemical Engineering and Light Industry, School of Biomedical and Pharmaceutical Sciences, Guangdong University of Technology, Guangzhou, Guangdong, 510006, China
[b] Department of Chemistry and Center of Super-Diamond and Advanced Films (COSDAF), City University of Hong Kong, 83 Tat Chee Avenue, Kowloon, Hong Kong, China
[c] Key Laboratory of Biochip Technology, Biotech and Health Centre, Shenzhen Research Institute of City University of Hong Kong, Shenzhen, 518057, China
[d] National Engineering Research Center for Tissue Restoration and Reconstruction, South China University of Technology, Guangzhou, 510006, China

ARTICLE INFO

Keywords:
Dual-quenching
Dual-reactive
HOCl
Ultra-sensitivity
Tissue imaging

ABSTRACT

We report herein fluorescent probes equipped with dual-quenching groups exhibiting superior sensitivity than probes with mono-quenching groups. Importantly, with this strategy, the probe with dual-quenching groups react with HOCl through two distinct reaction mechanisms, which reduce the plausible side reactions with other competing analytes and enhance the probe's selectivity. As a proof-of-concept study, we designed and synthesized a probe with dual-quenching groups **DQ-HOCl** to detect HOCl, which is one of the most important ROS and linked with a number of diseases. In addition, two control probes with mono-quenching groups, **MQ-HOCl-1** and **MQ-HOCl-2**, were also synthesized for comparison purpose. Fluorescent assays demonstrated that **DQ-HOCl** indeed shows ultra-high sensitivity and selectivity compared with probes with mono-quenching groups. Furthermore, the probe has been successfully utilized to imaging exogenous/endogenous HOCl in living cells. Moreover, **DQ-HOCl** was applied to visualize HOCl in kidney tissues from rat due to the increased penetration depth and lower tissue autofluorescence from the nature of two-photon probes.

1. Introduction

Small molecule fluorescent probes are powerful tools for detecting biologically relevant analytes in living cells or animals. These biologically relevant analytes include reactive oxygen species (ROS), reactive sulfur species (RSS), reactive nitrogen species (RNS), reactive carbonyl species (RCS), metal ions, pH, viscosity, carbohydrates, RNA, DNA, enzymes and others [1,2]. Designing novel fluorescent probe with high sensitivity and selectivity has attracted increasing attention in recent years. Developing such probes will not only aid in further elucidating the physiological and pathological roles of various analytes, but also facilitate early diagnosis of various diseases such as cancer and neurological diseases [3,4].

In general, a small molecule fluorescent probe consists of a fluorophore and a quencher, which quenches the fluorescence through different mechanisms, e.g. photoinduced electron transfer (PET), intramolecular charge transfer (ICT) and förster resonance energy transfer (FRET) [5–7]. Selecting an appropriate quencher for a specific probe is critical, since each quencher displays different chemical/electronic interactions with the fluorophore and affects the performance of the probe accordingly. Over the past decade, extensive efforts have been spent in developing fluorescent probes with ultra-high sensing ability. Nevertheless, most of the fluorescent probes suffer from low quenching effect, resulting in high fluorescence background and low sensitivity towards the targeting analyte. Consequently, designing highly sensitive fluorescent probes with novel quenching mechanism is

* Corresponding authors.
** Corresponding author at: Department of Chemistry and Center of Super-Diamond and Advanced Films (COSDAF), City University of Hong Kong, 83 Tat Chee Avenue, Kowloon, Hong Kong, China.
E-mail addresses: htzhang@gdut.edu.cn (H. Zhang), yjiang@gdut.edu.cn (Y. Jiang), hongysun@cityu.edu.hk (H. Sun).
[1] These authors have the equivalent contribution to this work.

https://doi.org/10.1016/j.snb.2020.127890
Received 26 October 2019; Received in revised form 28 January 2020; Accepted 17 February 2020
Available online 17 February 2020
0925-4005/

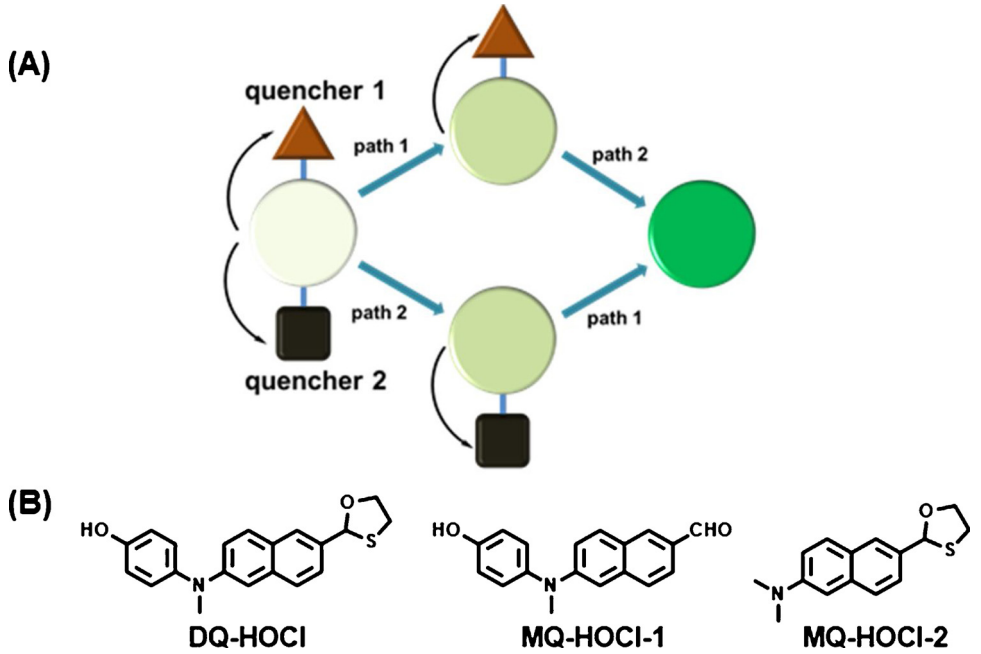

Scheme 1. (A) Schematic diagram of dual-reactive and dual-quenching probe; (B) Model probes for HOCl detection.

of strong demand and high importance.

HOCl is an important ROS and can be produced endogenously through myeloperoxidase (MPO)-catalyzed reaction of H_2O_2. Dysfunction of HOCl is linked with a number of diseases including cancers, neuron degeneration and cardiovascular diseases [8–10]. Due to its important role in living system, numerous fluorescent probes have been developed for detecting HOCl with low background and high sensitivity (Table S1) [11–35]. Despite these achievements, HOCl probes with superior sensitivity remains sparsely explored.

Herein, we present a facile and robust strategy to design HOCl fluorescent probes with superior sensitivity (Scheme 1A). Specifically, two reactive groups with different quenching mechanism were installed onto the same fluorophore concurrently. The two different quenching groups can quench the fluorescence in a synergetic manner. Hence the fluorescence background of the fluorophore can be reduced significantly. After reacting with HOCl, fluorescence increase will be significantly enhanced due to the minimized background [36–39]. On the other hand, the selectivity of the probe will also be improved because it contains two different reactive groups, which will react with HOCl through diverse reaction mechanisms and reduce the plausible side reactions with other competing analytes.

To prove our design concept, we designed and synthesized a series of HOCl probes, i.e. **DQ-HOCl**, **MQ-HOCl-1** and **MQ-HOCl-2** (Scheme 1B). In our design, *p*-hydroxyaniline and 1,3-oxathiolane group were chosen as the reactive groups. The two reactive groups can also serve as quenching groups. They have been reported by other groups for selective HOCl detection. In the case of **DQ-HOCl**, *p*-hydroxyaniline, due to its electron-rich property, quenches the fluorescence through PET process [40]. 1,3-oxathiolane, on the other hand, protects the aldehyde group on the naphthalene, reducing the electron pulling ability of the acceptor and resulting in fluorescence decrease [13]. For the fluorophore part, we chose 6-(methylamino)-2-naphthaldehyde, a donor-acceptor type two-photon fluorescent dye, which was used frequently for two photon imaging study [41–43]. We hypothesize that the fluorescence background of **DQ-HOCl** will be dramatically reduced through the synergistic quenching effect, whereas **MQ-HOCl-1** and **MQ-HOCl-2**, which possess single quenching group only, show higher fluorescence background and less sensitivity.

2. Experimental

2.1. Apparatus

^{1}H NMR and ^{13}C NMR spectra were taken on a Bruker 400 MHz NMR spectrometer. Mass spectra were recorded by PC Sciex API 150EX ESI-MS system and Thermo TSQ Endura Triple Quadrupole Mass Spectrometer. UV absorption spectra were obtained on Shimadzu UV-3600 Spectrophotometer. Fluorescence spectra were acquired with a FluoroMax-4 fluorescence photometer. Ultra-performance liquid chromatography (UPLC) were carried put on a Waters ACQUITY UPLC H-CLASS (H_2O-CH_3CN, from 40:60 to 10:90 in 5 min; flow rate: 0.2 mL/min; column: 2.1 × 50 mm). Two-photon fluorescence was excited by a fs laser (Spectra Physics, wavelength: 740 nm), and the spectrum was recorded with an optical fiber spectrometer (Ocean Optics). Fluorescence images were captured using a ZEISS LSM 800 With Airscan Confocal Laser Scanning Microscope and Leica TCS SP5 Confocal Scanning Microscope.

2.2. Reagents

All chemicals used for synthesis were purchased from commercial suppliers and applied directly without purification. 6-hydroxy-2-naphthaldehyde, TBSCl, imidazole, Cs_2CO_3 and $Pd(OA_C)_2$ were obtained from J&K Chemical. Dimethylamine, $Na_2S_2O_5$, dimercaptoethanol, were bought from Titan Co.. 6-bromo-2-naphthaldehyde, BINAP were purchased from Bidepharm. TMSOTf, 4-methylamino-phenol sulfate were obtained from Energy Chemical. Anhydrous dichloromethane (DCM), toluene, and tetrahydrofuran (THF) were purchased from Adamas-beta® and used in all reaction as solvent. Dulbecco's modified Eagle's medium (DMEM), PBS, fetal bovine serum (FBS), trypsin-EDTA and penicillin/streptomycin were purchased from Invitrogen. All reactions that utilize air- or moisture sensitive reagents were performed in dried glassware under dry argon atmosphere. Milli-Q water was used in all experiments.

2.3. Synthesis of the compounds

DQ-HOCl, **MQ-HOCl-1**, **MQ-HOCl-2, DQ-1, DQ-2 and DQ-1-OCl** were synthesized through established procedure and obtained with

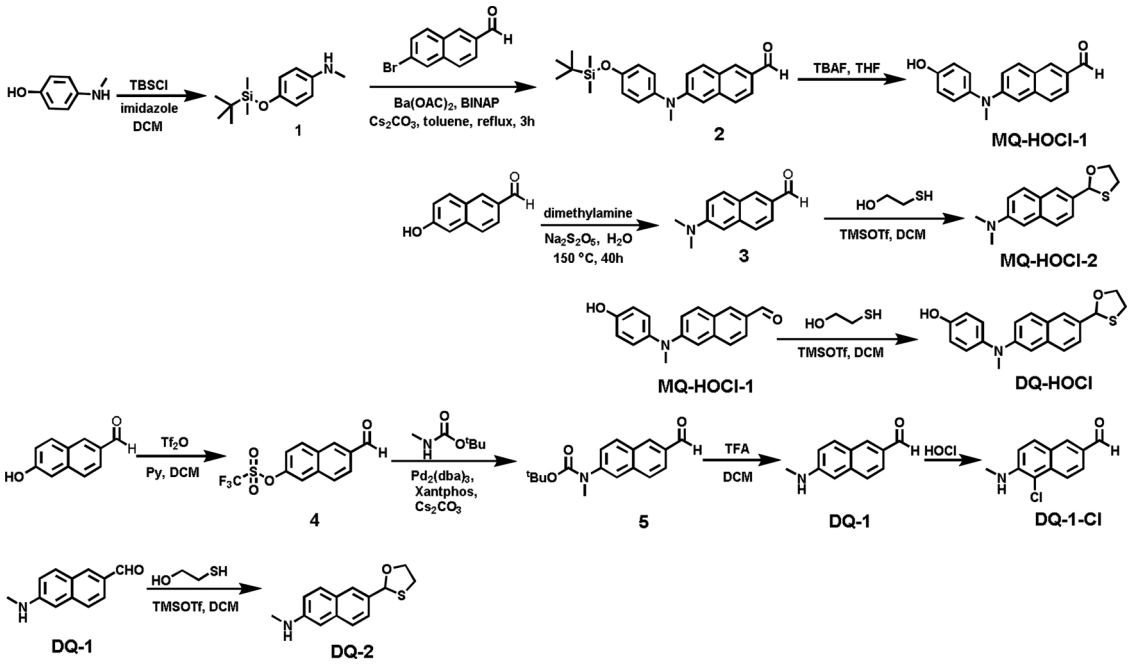

Scheme 2. The synthetic route for **MQ-HOCl-1**, **MQ-HOCl-2, DQ-1, DQ-2, DQ-1-Cl** and **DQ-HOCl**.

good yields (Scheme 2). All the compounds were characterized by ^{1}H NMR, ^{13}C NMR and ESI-MS and all the characterizations have been shown in Supporting Information.

2.4. Absorption and fluorescence measurement

MQ-HOCl-1, **MQ-HOCl-2** and **DQ-HOCl** were dissolved in an appropriate amount of DMF to obtain 3 mM or 10 mM stock solution. Cys and GSH were prepared as 200 mM stock solutions in PBS buffer (pH 7.4, 100 mM). $NaNO_3$, $NaNO_2$, $FeCl_3$, $FeCl_2$, KCl were prepared as 50 mM stock solutions in water. Hydroxyl radical (•OH) was generated by reaction of 1 mM Fe^{2+} with 200 μM H_2O_2 [44]. Superoxide was generated from KO_2, which was dissolved in DMSO with 18-crown-6 ether (2.5 eq) to afford a 250 μM solution [45]. $ONOO^-$ were prepared with KNO_2, HC1, H_2O_2 and NaOH. Generally, KNO_2 (1.2 M) was mixed with H_2O_2 (1.4 M) and HC1 (1.2 M) at 0 °C, and NaOH (3.0 M) was added immediately after the three compounds were mixed to make the solution alkaline. Excess H_2O_2 was removed by passing the solution through a short column of MnO_2 [46]. Finally, all the concentrations of ROS were determined from the absorption experiment followed from the protocol of Nagano's group by Beer-Lambert Law with UV absorption [47]. Specifically, the extinction coefficient (ε) of H_2O_2, -OCl, and ONOO- were 43.6 M^{-1} cm^{-1}, 350 M^{-1} cm^{-1} and 1670 M^{-1} cm^{-1} respectively. The determined absorption was at 240 nm, 292 nm and 302 nm for H_2O_2, -OCl, and ONOO-.

All the measurement was taken under room temperature. Firstly, **MQ-HOCl-1**, **MQ-HOCl-2** or **DQ-HOCl** was diluted in PBS buffer (pH 7.4, 10 mM) to afford a final concentration of 1 μM in a 10-mm quartz cuvette. Then, different concentrations of NaOCl or other analytes were added into the quartz cuvette for 1 min incubation respectively. After that, the absorption or fluorescence was measured using Shimadzu 1700 UV/vis Spectrometer and FluoroMax-4 fluorescence photometer respectively.

2.5. Cell culture and confocal fluorescence imaging

WI38 cells, B16F10 cells and RAW 264.7 macrophage cells were cultured in Dulbecco's modified Eagle's medium (DMEM) supplemented with 10 % fetal bovine serum (FBS) and 1% antibiotics (penicillin and streptomycin).

For exogenous HOCl fluorescence imaging, the cells were seeded in a glass-bottomed confocal dish (35 mm) with a density of approximately $1*10^5$ cells/mL. After 24 h, the cells were treated with **DQ-HOCl** (5 μM) at 37 °C for 30 min and then incubated with NaOCl (50 μM) for another 20 min. Fluorescence images were taken using a ZEISS LSM 800 With Airscan Confocal Laser Scanning Microscope.

For endogenous HOCl fluorescence imaging, RAW 264.7 macrophage cells were seeded in a glass-bottomed confocal dish (35 mm) with a density of approximately $1*10^5$ cells/mL. After 24 h, the cells were treated with LPS (2 μg/mL)/PMA (2 μg/mL) for 2 h. Then, **DQ-HOCl** (5 μM) were added into the dishes as well for 20 min incubation. After washing with DPBS twice, fluorescence images were taken using a ZEISS LSM 800 With Airscan Confocal Laser Scanning Microscope. Cells treated with **DQ-HOCl** (5 μM) alone were used as a control experiment. As to the negative control, the cells were pre-treated with LPS (2 μg/mL)/PMA (2 μg/mL)/ ABH (200 μM) for 2 h. Then, **DQ-HOCl** (5 μM) were added into the dishes as well for 20 min incubation. After washing with DPBS twice, fluorescence images were taken using a ZEISS LSM 800 With Airscan Confocal Laser Scanning Microscope. Ex: 405 nm, Em: 450 − 550 nm.

2.6. Two-photon imaging of fresh tissue

Kidney slices were obtained from three-week-old rat. The tissues were cut into thickness of 400 μm slices using a vibrating-blade microtome in artificial cerebrospinal fluid. The tissue slices were incubated with HOCl (100 μM) for 1 h, and washes wish PBS for two times. Then the tissue slices were incubated with **DQ-HOCl** (10 μM) for 1 h at 37 °C. Following that the slices were washed two times and transferred into a confocal culture dish. Imaging was performed using Leica TCS SP5 Confocal Scanning Microscope with 40X oil objectives under multiphoton excitation at 720 nm. The fluorescent emission window was set from 450 − 550 nm.

3. Result and discussion

3.1. The possible reaction mechanism

To examine the response mechanism of **DQ-HOCl**, reversed-phase UPLC was used to analyze the reaction between **DQ-HOCl** and HOCl. We first measured the retention time for **DQ-1**, **MQ-HOCl-1**, **DQ-1-Cl** and **DQ-HOCl** using UPLC. Their retention time is determined to be 1.03 min, 1.35 min, 1.65 min and 2.11 min respectively (Fig. S1). When **DQ-HOCl** was treated with 2 eq. of HOCl, three peaks belonging to MQ-HOCl, **DQ-1-Cl** and **DQ-HOCl** were observed, indicating that the reaction was not complete and **MQ-HOCl-1** was the intermediate product during the reaction. When the concentration of HOCl was increased to 4 eq, the peak of **DQ-1** became the major product, signifying that **MQ-HOCl-1** reacted with HOCl completely. However, when 6 eq. of HOCl was used for the reaction, only the major peak of **DQ-1-Cl** could be observed, indicating **DQ-1** could be chlorinated.

For the position of chlorine atom of **DQ-1-Cl**, we performed detailed characterization experiments with ^{1}H NMR, ^{13}C NMR and ESI-MS. Through thorough analysis, we reckon that chlorination occurs at C-5 position (Fig. S40, S41 and S48). The conclusion is also supported by reports from our group and other groups [19,48].

From the above experiments, we propose that the reaction mechanism of **DQ-HOCl** and HOCl follows Scheme 3: **DQ-HOCl** itself is non-fluorescent because of the quenching effect of intramolecular charge transfer (ICT) and photoinduced electron transfer (PET) by 1,3-oxathiolane group and *p*-hydroxyaniline group. When **DQ-HOCl** reacts with HOCl, the sulfur atom is first oxidized to sulfoxide by HOCl. The sulfoxide intermediate can then be further oxidized to form sulphone compound, which is unstable and hydrolyzed rapidly. The hydrolyzed product, **MQ-HOCl-1**, reacts with HOCl sequentially and generates fluorescent compound **DQ-1**. Finally, **DQ-1** is chlorinated by HOCl to produce **DQ-1-Cl**, which is also fluorescent.

To elucidate the fluorescence 'off-on' process of the probe using computational chemistry method, frontier molecular orbital energies of **DQ-HOCl** and **DQ-1** were calculated according to the reported method using Gaussian 09 (DFT/TDDFT in B3LYP/6 − 31 G level) [49,50]. The calculated results indicated that the oscillator strength (*f*) of **DQ-HOCl** for the electron transition from HOMO to LUMO is only 0.0017, signifying that electron transition from HOMO to LUMO is prohibited (Fig. S2A). Therefore, electronic transition from the excited state to the ground state cannot occur, and the fluorescence is in 'off' state. After reacting with HOCl, **DQ-HOCl** turns into **DQ-1**. The oscillator strength of **DQ-1** for the electron transition from HOMO to LUMO changes to 0.6723, indicating that electron transition from HOMO to LUMO is allowed and fluorescence is in 'on' state (Fig.S2B).

3.2. Optical properties of probes towards HOCl

After confirming the chemical structures of the probes, preliminary absorption and fluorescence emission study was carried out. As shown in Fig. 1A and S3, after reacting with HOCl, **MQ-HOCl-1** displayed moderate decrease at 385 nm in the absorption spectra. However, **MQ-HOCl-2** showed an absorption shift from 294 nm to 357 nm, which is the typical phenomenon of ICT quenching mechanism (Fig. 1C and S4) [51,52]. **DQ-HOCl** showed similar absorption shift as **MQ-HOCl-2**, but the absorbance signal did not increase as sharply as **MQ-HOCl-2** (Fig. 1E and S5). In fluorescence test, after reacting with HOCl, a clear signal increase could be observed for **MQ-HOCl-1** (Fig. 1B). For **MQ-HOCl-2**, an inconspicuous ratiometric wavelength shift from 433 nm to 530 nm was found (Fig. 1D). The background intensity of **MQ-HOCl-2** at 530 nm is quite obvious. Moreover, a clear fluorescence change of blue to green was observed under excitation of a handheld UV lamp (insert figure in Fig. 1C). For **DQ-HOCl**, only fluorescence turn-on effect was observed with the maximum emission peak at 518 nm (Fig. 1F). These results prove that all three probes can react with HOCl as designed and show different behaviours in reacting with HOCl. It is noted that DMSO cannot be used to dissolve the probes for preparation of stock solution because DMSO could react with HOCl and interfere the

Sensitivity and detection limit

Next, we investigated the sensitivity of the three probes by reacting with various concentrations of HOCl. As shown in Fig. 2, **MQ-HOCl-1** responded to 1 μM HOCl sensitively with a 37-fold fluorescence increase (Fig. 2A). For **MQ-HOCl-2**, despite ratiometric enhancement, the ratio of fluorescence intensity only changed by 12-fold with 1 μM HOCl (Fig. 2B). **DQ-HOCl**, as predicted, showed a striking fluorescence enhancement of 244-fold, which is much higher than **MQ-HOCl-1** and **MQ-HOCl-2** (Fig. 2C). Detailed fluorescence ratio changes (F/F_0) before and after reaction with HOCl is provided in Fig. 2D. Similar result was obtained in the range of 0 − 10 μM HOCl, and over 8000-fold increase was observed with **DQ-HOCl** and 10 μM HOCl (Fig. S9). The sensitivity results with the three probes prove that our design strategy of installing two quenching groups can significantly increase the probe's sensitivity.

We then performed more detailed sensitivity study with **DQ-HOCl**. Lower concentration of HOCl was used in the titration experiment. As depicted in Fig. S10, the fluorescence intensity of **DQ-HOCl** at 518 nm shows a linear correlation with HOCl concentration in the range of 0 − 500 nM. Remarkably, a 22-fold and 135-fold fluorescence increase was obtained with 100 nM and 500 nM HOCl respectively, indicating the high chance to detect trace amounts of HOCl in the living cells (Fig. S10). In addition, the detection limit of **MQ-HOCl-1**, **MQ-HOCl-2** and **DQ-HOCl** are determined to be 41.9 nM, 85.8 nM and 3.5 nM based on the equation of $3\sigma/\kappa$ (Table S2). These results again demonstrate **DQ-HOCl** possesses ultra-sensitivity towards HOCl.

3.3. Kinetics

The lifetime of HOCl is short in biological environment. Consequently, it is important to investigate detailed kinetics of the probes reacting with HOCl. A significant time-dependent fluorescence

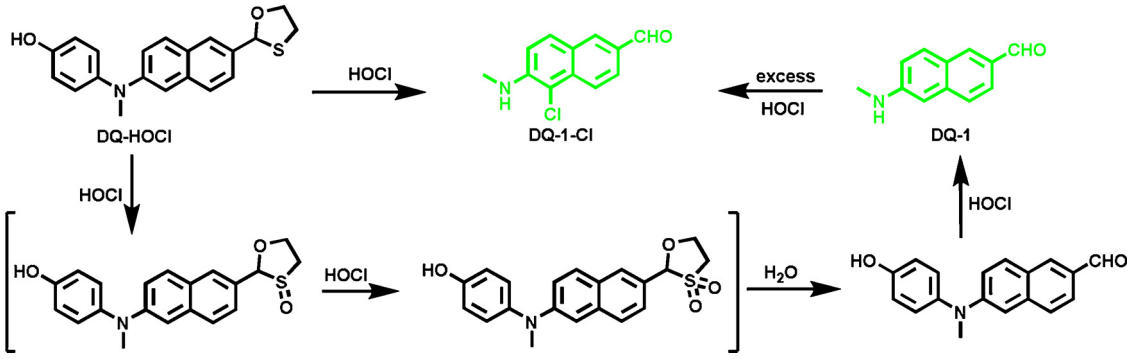

Scheme 3. The proposed reaction mechanism of **DQ-HOCl** towards HOCl., experiment result (Fig. S6-S8).

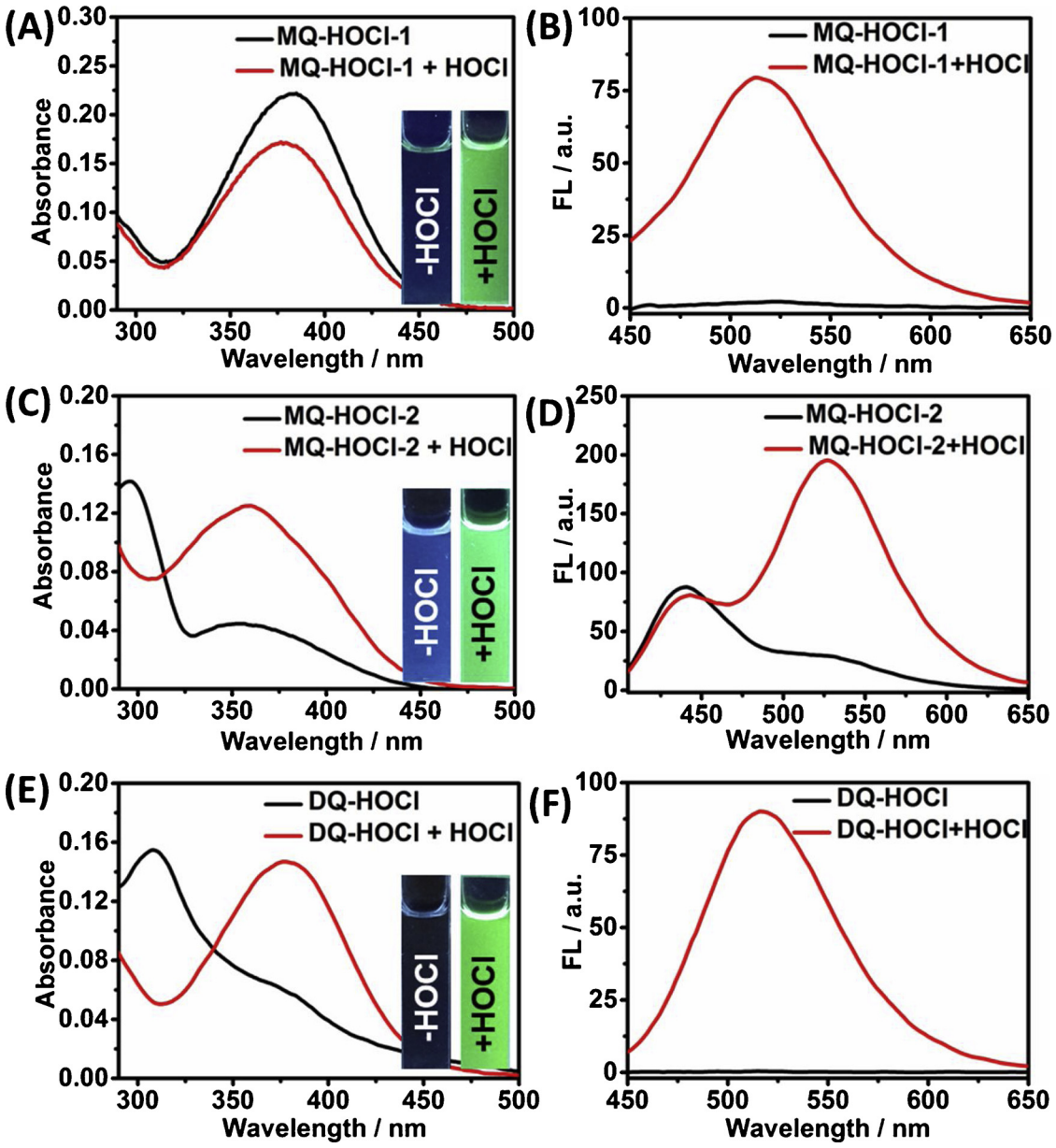

Fig. 1. Absorption and emission spectra of **MQ-HOCl-1** (A and B), **MQ-HOCl-2** (C and D) and **DQ-HOCl** (E and F) in the absence and presence of HOCl in PBS buffer (pH 7.4, 10 mM). For absorption experiment, probes concentration was 10 μM and HOCl was 40 μM. For emission spectra, probes concentration was 1 μM, HOCl was 1 μM. The insert pictures: fluorescence changes in the absence and presence of HOCl under a hand-held UV lamp, Probes: 50 μM, HOCl: 100 μM.

enhancement of **MQ-HOCl-2** and **DQ-HOCl** towards HOCl could be observed (Fig. 3A and 3B). In addition, the fluorescence intensities of probes and the reaction products remained unchanged in the solution, indicating that both probes possess excellent stability. However, the stability of **MQ-HOCl-1** turns out not as good as the other two probes. As shown in Fig. 3C and S11, the fluorescence intensity of **MQ-HOCl-1** showed a gradual increase in PBS buffer. This result indicates that **MQ-HOCl-1** is prone to hydrolysis and may not be suitable for further biological applications. Furthermore, we also tested the reactivity of **DQ-HOCl** towards MPO, which catalyses H_2O_2 and Cl^- to generate HOCl in situ [48,53]. As shown in Fig. 3D, **DQ-HOCl** reacts rapidly in the presence of MPO, H_2O_2 and Cl^-. With lower concentration of MPO, the reaction kinetic decreases as well, signifying that MPO is the key enzyme to produce HOCl. The experiment also suggests that **DQ-HOCl** has high selectivity towards HOCl rather than towards other ROS, such as H_2O_2. These results together demonstrate that **DQ-HOCl** is capable of monitoring the enzymatic activity of MPO in real time.

3.4. Selectivity

We next examined the selectivity of the three probes more extensively. The three probes were treated with various analytes, such as Cys and GSH from RSS group, TBHP, ·OH, $O_2^{\cdot -}$, H_2O_2 and ONOO- from ROS group, NO_2- and NO_3- from RNS group, Fe^{2+}, Fe^{3+}, and K^+, and the fluorescence response was provided in Fig. 4 and Fig. S11-S13. Among the three probes, **MQ-HOCl-1** is interfered by ONOO-, which showed a 76-fold fluorescence increase reacting with 5 μM ONOO- and a 37-fold fluorescence increment reacting with 1 μM HOCl (Fig. 4 & S12). For **MQ-HOCl-2**, although the selectivity is not as poor as **MQ-HOCl-1**, the fluorescence increment to all analytes is not very high (Fig. 1B & S13). **DQ-HOCl** displayed the highest selectivity ratio upon treatment with HOCl (Fig. S14). More specifically, the fluorescence spectra response of **DQ-HOCl** with different concentrations of analytes was monitored carefully (Fig. S15). No obvious fluorescence change was observed when **DQ-HOCl** was incubated with incremental

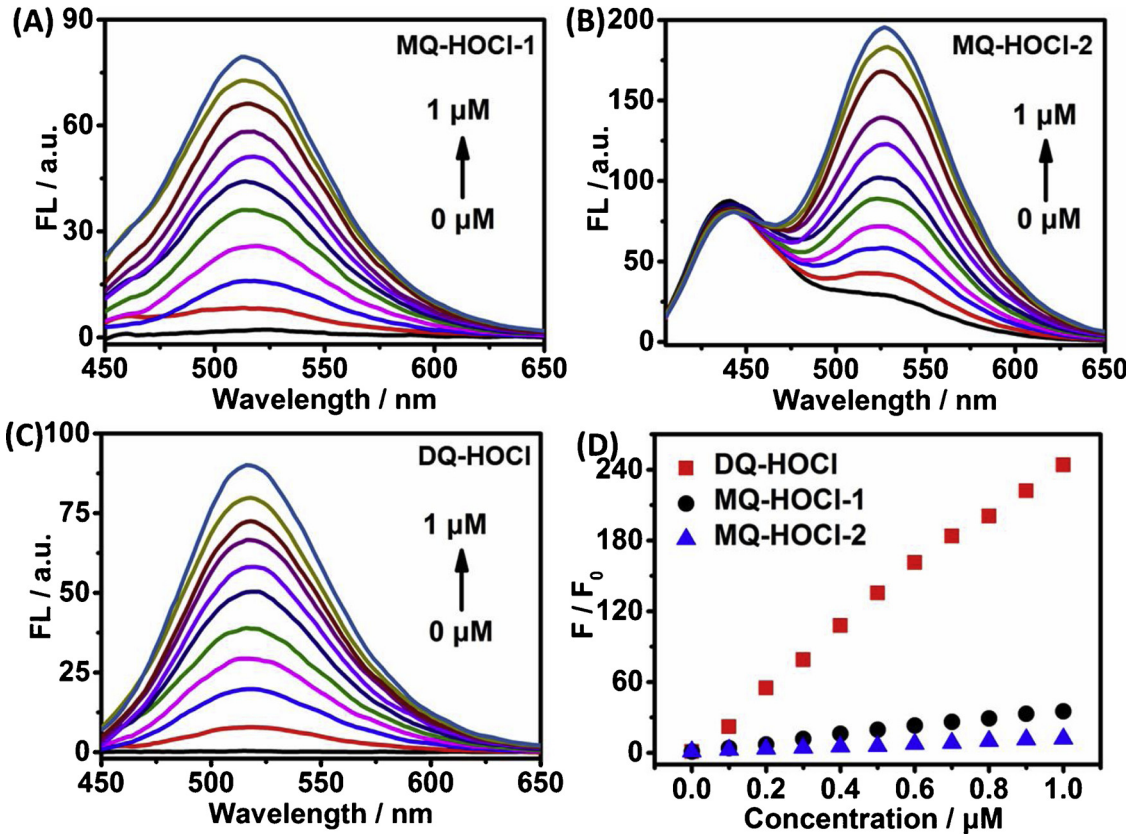

Fig. 2. Fluorescence spectra of **MQ-HOCl-1** (1 μM) (A), **MQ-HOCl-2** (1 μM) (B) and **DQ-HOCl** (1 μM) (C) towards various concentration of HOCl (0-1 μM) in PBS buffer (pH 7.4, 10 mM); (D) Plot of fluorescence intensity ratio changes (F/F_0) of probes. For **MQ-HOCl-1** and **DQ-HOCl**, F/F_0 is the ratio of fluorescence intensity at 518 nm. For **MQ-HOCl-2**, F/F_0 is the fluorescence intensity ratio of I_{530}/I_{433}. λex = 395 nm.

concentrations of other analytes except HOCl. These results imply that **DQ-HOCl** has high selectivity towards HOCl and might possess excellent biocompatibility in complex cellular environment.

We have also analyzed the reaction of **DQ-HOCl** and **MQ-HOCl-1** with $ONOO^-$ respectively by UPLC. As shown in Fig. S16, **MQ-HOCl-1** displayed reactivity with $ONOO^-$ and produced fluorescent compound **DQ-1**, which could interfere with the detection of HOCl. In the case of **DQ-HOCl**, it also reacted with $ONOO^-$ in PBS buffer (Fig. S17). However, the reaction product was **DQ-2**, which showed almost no fluorescence because 1,3-oxathiolane group quenched the fluorescence. This allows **DQ-HOCl** to detect HOCl with high selectivity. It cannot be achieved by **MQ-HOCl-1**. The experiment results also verified the superior performance of the probe design with dual-quenching groups to reduce the interference of other biological molecules.

Based on the above data, we want to further discuss about the selectivity of **MQ-HOCl-1** and **DQ-HOCl** towards HOCl and $ONOO^-$ by fluorescence method. Some literatures have reported that *p*-hydroxyaniline is a much more sensitive group to $ONOO^-$ than HOCl [54,55]. We tested the kinetic behaviour between **MQ-HOCl-1** and ONOO- firstly. As shown in Fig. S18, **MQ-HOCl-1** shows fast reaction kinetic with ONOO- in 1 min as well as with HOCl. However, **DQ-HOCl** did not show any fluorescence response with ONOO- even after long time incubation. Next we investigated the sensitivity of **MQ-HOCl-1** to different concentration of $ONOO^-$ (1 − 10 μM) more carefully. As shown in Fig. S19A, the fluorescence intensity increased gradually with the incremental concentration of $ONOO^-$ after 1 min incubation in the range of 1 − 7 μM. Therefore, we conclude that **MQ-HOCl-1** is not suitable for selective HOCl detection as it could react with ONOO-. As to **DQ-HOCl**, no obvious fluorescence can be observed after reacting with different concentration of $ONOO^-$ (1 − 10 μM) (Fig. S19B & 19C). This result is a perfect demonstration that using two different reactive/quenching groups can provide enhanced selectivity even if one of the reactive/quenching group is interfered by other analytes. Combining the above selectivity result with the MPO experiment data, which generates HOCl in situ, it is confirmed clearly that **DQ-HOCl** provide much higher selectivity than **MQ-HOCl-1** and **MQ-HOCl-2**.

3.5. pH effect

We have investigated the pH effect on the response of the three probes to HOCl. For the reaction of **MQ-HOCl-2** and HOCl, a remarkable fluorescence increase could be observed after treatment of HOCl. The fluorescence did not change significantly over a wide pH range (4–10) (Fig. S20B). The other two probes, **MQ-HOCl-1** and **DQ-HOCl**, whose structures have the phenolic hydroxyl group, showed the distinctively different result. The fluorescence intensity of the two reaction buffers increased from pH 4 to pH 7 and reached the maximum at pH 7. Subsequently the fluorescence intensity decreased when pH value changed from 7 to 10 (Fig. S20A & S20C). These results agree with the reported literature [56]. Taken together, the pH experiments suggest that the three probes can be used to detect HOCl across a wide range of pH values. **MQ-HOCl-1** and **DQ-HOCl** have a preferable pH of around 7.

3.6. Biological imaging application in living cells

Subsequently, we investigated whether **DQ-HOCl** can be applied to live cell imaging studies. MTT test was performed to evaluate the cytotoxicity of **DQ-HOCl** [57,58]. As shown in Fig. S21, 20 μM **DQ-HOCl** exhibits low cytotoxicity, with over 90 % of B16F10 cells survived after 24 h of incubation. The low cytotoxicity of **DQ-HOCl** encouraged us to apply **DQ-HOCl** to further imaging exogenous and endogenous HOCl in

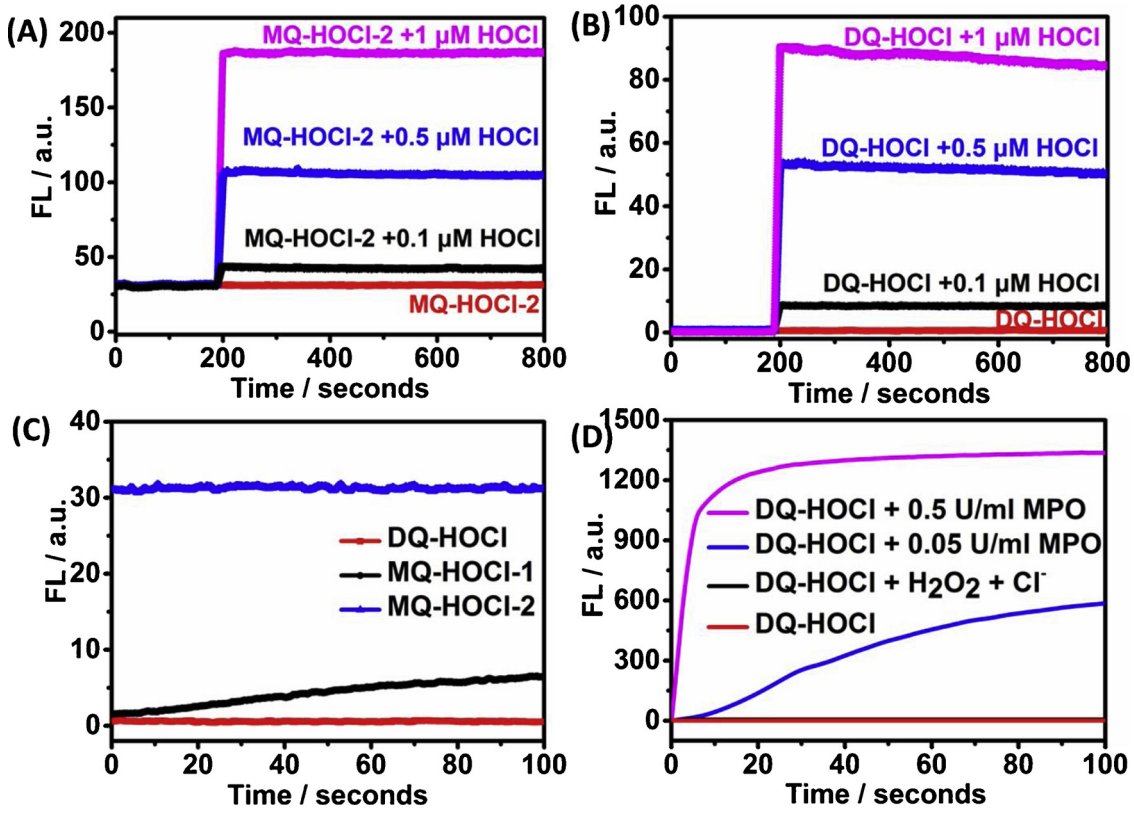

Fig. 3. Time-dependent fluorescence intensity changes of **MQ-HOCl-2** (1 μM) (A) and **DQ-HOCl** (1 μM) (B) in the absence and presence of HOCl in PBS buffer (pH 7.4, 10 mM), For **MQ-HOCl-2**, the Y-axis represents the fluorescence intensity ratio of I_{530}/I_{433}. For **DQ-HOCl,** the Y-axis represents the intensity at 518 nm; (C) The stability test of **MQ-HOCl-1**, **MQ-HOCl-2** and **DQ-HOCl** by monitor the fluorescence intensity at 518 nm using continuous laser excitation in PBS buffer; (D) Fluorescence responses of **DQ-HOCl** towards HOCl generated in the system of MPO/H_2O_2/Cl^-. H_2O_2: 100 μM, Cl^-: 100 μM. λex = 395 nm.

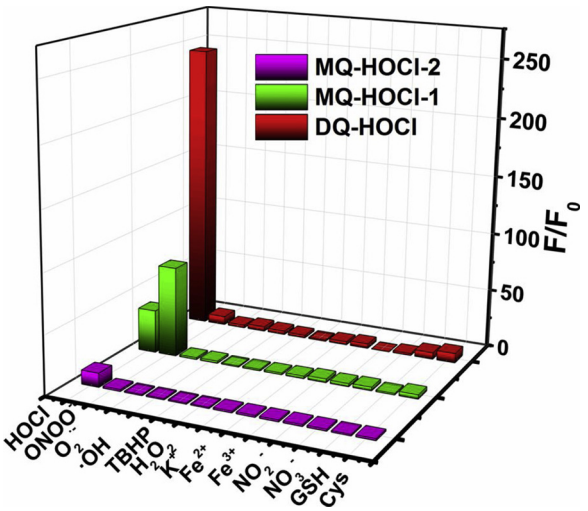

Fig. 4. Selectivity of **MQ-HOCl-1** (1 μM), **MQ-HOCl-2** (1 μM) and **DQ-HOCl** (1 μM) by monitoring the fluorescence intensity ratio in PBS buffer (pH 7.4, 10 mM). For **MQ-HOCl-1** and **DQ-HOCl**, F/F_0 is the ratio of fluorescence intensity at 518 nm. For **MQ-HOCl-2**, F/F_0 is the fluorescence intensity ratio of I_{530}/I_{433}. For Cys and GSH, the concentration is 5 mM. For NO_2^-, NO_3^-, Fe^{2+}, Fe^{3+}, K^+, TBHP, ·OH, $O_2^{\cdot-}$, H_2O_2, the concentration is 50 μM. For $ONOO^-$, the concentration is 5 μM. For HOCl, the concentration is 1 μM. λex = 395 nm.

living cells. In addition, we also investigated the solubility of the reaction product in aqueous solution, as it will affect the imaging performance in living cells. We tested the solubility of the reaction product by fluorescence test in the range of 1 − 60 μM according to the literature's method [59,60]. As shown in Fig. S22, the solubility is determined as 15 μM by fluorescence method, which is sufficient enough for live cell imaging.

To conduct exogenous HOCl imaging studies, B16F10 and WI38 cells, which belong to metastatic melanoma cell line and human lung fibroblast cell line respectively, were chosen in our study. Cells were incubated separately with **DQ-HOCl** (5 μM) at 37 ˚C for 20 min. HOCl (50 μM) was then added to the cells and incubated for another 20 min. As depicted in Fig. 5A and 5C, the cells show obvious fluorescence increase under confocal imaging microscopy, suggesting **DQ-HOCl** is cell permeable and can selectively respond to HOCl in complex cellular environment.

In endogenous HOCl imaging, Raw 264.7 mouse macrophages was chosen because of its ability to generate endogenous HOCl after stimulation with lipopolysaccharide (LPS) and phorbol myristate acetate (PMA) [56,61,62]. As shown in Fig. 5B1-5B2, the cells showed slight green fluorescence after incubated with **DQ-HOCl** for only 20 min. The result indicates that Raw 264.7 cells can generate low concentration of HOCl by itself without any stimulation. Next, RAW 264.7 was stimulated with LPS and PMA to produce more HOCl endogenously. As predicted, much higher fluorescence intensity was observed after stimulation (Fig. 5B3-B4). Furthermore, 4-aminobenzoic acid hydrazide (ABH), which can decrease the generation of endogenous HOCl through inhibiting the activity of MPO, was used in the control experiment [19,63–65]. No observable fluorescence can be found in the experiments with LPS/PMA/ABH treatment, confirming the turn-on fluorescence is attributed to the selective reaction between **DQ-HOCl** and endogenous HOCl in cells (Fig. 5B5-5B6).

3.7. *Two-photon imaging of HOCl in fresh tissues*

Inspired by the capability of exogenous and endogenous HOCl

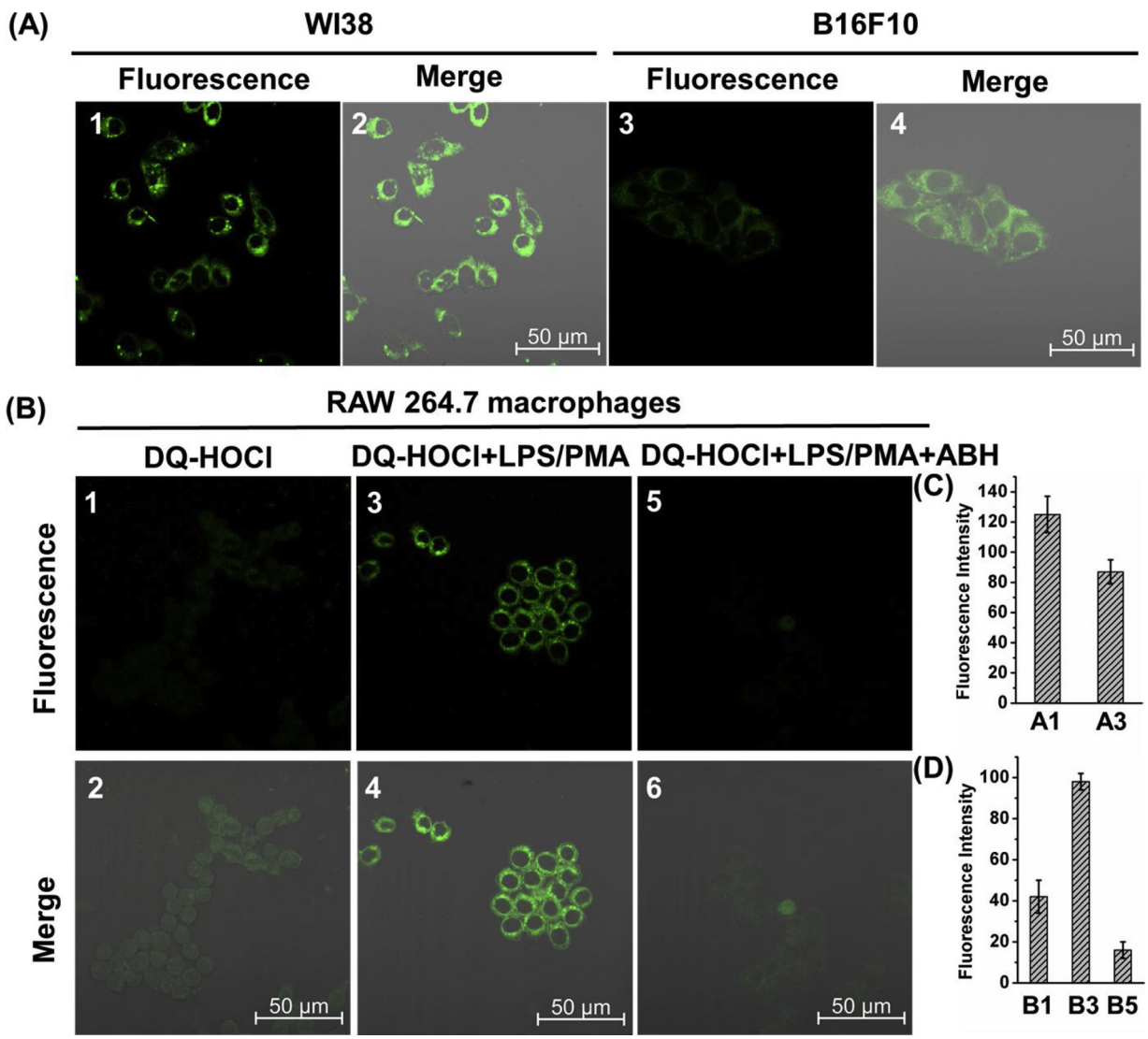

Fig. 5. (A) Fluorescence confocal microscopy images of WI38 (A1-A2) and B16F10 (A3-A4) incubated with **DQ-HOCl** (5 μM) for 20 min and then with HOCl (50 μM) for another 20 min. (B) Detection of endogenous HOCl produced by LPS/PMA in macrophage. B1-B2: **DQ-HOCl** only (5 μM); B3-B4: cells were treated with LPS (2 μg/mL)/PMA (2 μg/mL) for 2 h, then incubated with **DQ-HOCl** (5 μM) for another 20 min; B5-B6: cells were treated with LPS (2 μg/mL)/PMA (2 μg/mL)/ABH (200 μM) for 2 h, then incubated with **DQ-HOCl** (5 μM) for another 20 min. (C) Relative fluorescence intensity of cells in Fig. 5A. (D) Relative fluorescence intensity of cells in Fig. 5B. Ex: 405 nm, Em: 450-550 nm.

imaging in living cells, we then investigated the capability of **DQ-HOCl** to detect HOCl in the tissues by two-photon fluorescence imaging. Two photon action cross-section of the reaction was first investigated. As shown in Fig. S23, in the range of 700−880 nm, the maximum two-photon absorption cross-section of the reaction between **DQ-HOCl** and HOCl was determined to be 72 GM at 740 nm. This value is similar to that of two-photon dyes with similar structures [66,67]. In addition, we studied the fluorescence intensity (I_{out}) as a function of the excitation laser power (I_{in}) on a log-log scale [68–72]. As shown in Fig. S24, the slope of the plot was determined to be 1.88, which is close to 2.0, indicating that the fluorescence was produced by two-photon excitation. These two-photon experiments demonstrated that **DQ-HOCl** has strong potential to be applied to two photon biological imaging.

Literatures have shown that polymorphonuclear- and monocyte-derived ROS (including HOCl) may lead to the development of atherosclerosis through oxidative modification of proteins, lipids, and nucleic acids in glomerular oxidative killing, cause dysfunction of cells in different compartments of the kidney [73,74]. Therefore, the tissue slices of rat living kidney were prepared and used for two-photon imaging study. The tissues slices were first treated with HOCl (100 μM) for 1 h followed by three time washing. Then, the tissues slices were incubated with **DQ-HOCl** (10 μM) for 1 h as well. As shown in Fig. 6 and S25, **DQ-HOCl** exhibits good imaging performance for HOCl detection at various sample depths (> 240 μm) using the z-scan mode of a confocal microscope. The movie, which shows the two-photon fluorescence changes with different slices depth, has also proved that the capability of deep tissue penetration, high sensitivity and low background fluorescence of **DQ-HOCl** (Shown in Movie S1).

4. Conclusions

In summary, we have constructed an ultra-sensitive HOCl probe using a robust strategy by introducing two quenching groups to the same fluorophore. The resulting probe exhibited enhanced sensitivity and selectivity in detecting HOCl. To prove the concept, three fluorescent probes, **MQ-HOCl-1**, **MQ-HOCl-2** and **DQ-HOCl**, have been designed and synthesized for HOCl detection. Because of the orthogonality of the two quencher groups, 1,3-oxathiolane group and *p*-hydroxyaniline group, the background fluorescence of **DQ-HOCl** was reduced greatly, resulting in superior sensitivity of **DQ-HOCl** towards

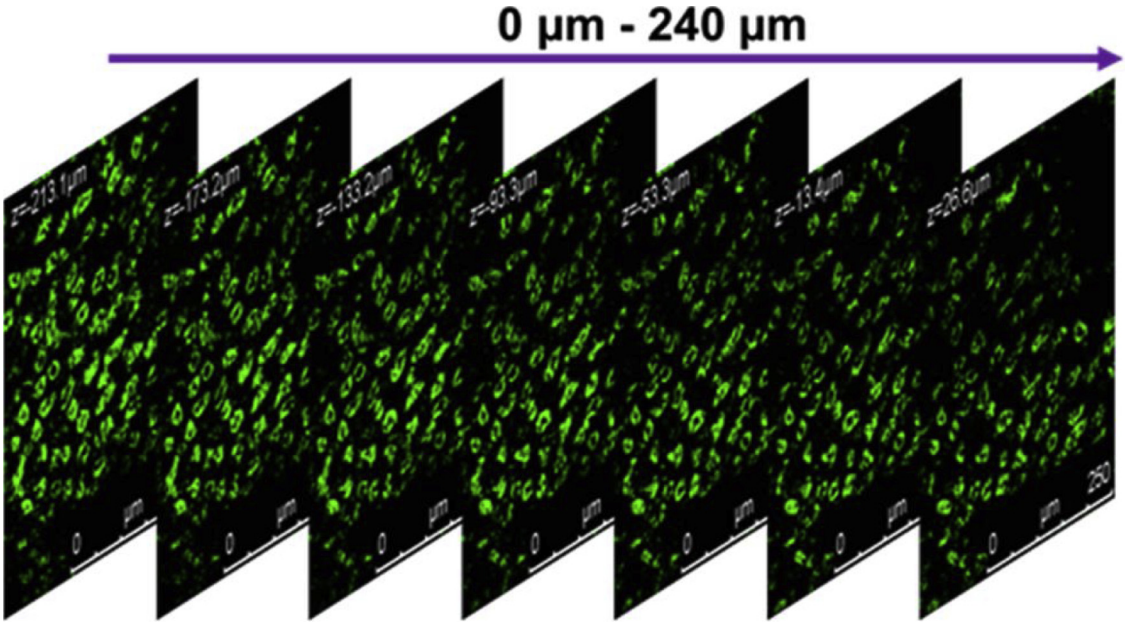

Fig. 6. Two-photon confocal images of HOCl probe taken from a series of fresh rat kidney slice incubated with 10 μM **DQ-HOCl** and HOCl with magnification at 40 × . Ex: 720 nm, Em: 450-550 nm.

HOCl. In addition, due to the two orthogonal quencher groups, the selectivity of **DQ-HOCl** was proven better compared with **MQ-HOCl-1**. It is noted that **DQ-HOCl** reacted with the interfering substance, $ONOO^-$ through one quenching group. However, the left quenching group, 1,3-oxathiolane, can still quench the fluorescence by ICT effect. As a result, **DQ-HOCl** exhibits enhanced selectivity towards HOCl than **MQ-HOCl-1.** Importantly the reaction mechanism of **DQ-HOCl** with HOCl has been verified by fluorimeter, UPLC, ^{1}H NMR, ^{13}C NMR and ESI-MS. Furthermore, we have successfully applied **DQ-HOCl** to imaging HOCl in different cell lines and rat kidney tissue. Based on our experimental results, we envision that the concept of dual-quenching groups can inspire the development of many new probes with enhanced sensitivity and selectivity. Such probes will find useful applications in detecting many biologically important analytes in living systems.

Declaration of Competing Interest

There are no conflicts to declare.

Acknowledgments

We appreciate the help from Mrs. Xiao Zhou in GDUT Analysis and Test Center for confocal imaging work. This work was supported by the National Natural Science Foundation of China (No. 21807014, 21602033, 21572190), Shenzhen Basic Research Project (JCYJ20180507181654823), the Pearl River Talent Plan of Guangdong Province (2017GC010596), Guangxi Natural Science Foundation (2016GXNSFBA380123), the Hong Kong Research Grants Council (11302415 and 11334516) and the City University of Hong Kong grant (9667147).

Appendix A. Supplementary data

Supplementary material related to this article can be found, in the online version, at doi:https://doi.org/10.1016/j.snb.2020.127890.

References

[1] M.E. Jun, B. Roy, K.H. Ahn, "Turn-on" fluorescent sensing with "reactive" probes, Chem. Commun. 47 (2011) 7583–7601.
[2] Z. Guo, S. Park, J. Yoon, I. Shin, Recent progress in the development of near-infrared fluorescent probes for bioimaging applications, Chem. Soc. Rev. 43 (2014) 16–29.
[3] X. Zhen, J. Zhang, J. Huang, C. Xie, Q. Miao, K. Pu, Macrotheranostic probe with disease-activated near-infrared fluorescence, photoacoustic, and photothermal signals for imaging-guided therapy, Angew Chem. Int. Edit. 57 (2018) 7804–7808.
[4] M.J. Landau, D.J. Gould, K.M. Patel, Advances in fluorescent-image guided surgery, Ann. Transl. Med. 4 (2016) 392-392.
[5] H.-W. Liu, L. Chen, C. Xu, Z. Li, H. Zhang, X.-B. Zhang, W. Tan, Recent progresses in small-molecule enzymatic fluorescent probes for cancer imaging, Chem. Soc. Rev. 47 (2018) 7140–7180.
[6] L. Yuan, W. Lin, K. Zheng, L. He, W. Huang, Far-red to near infrared analyte-responsive fluorescent probes based on organic fluorophore platforms for fluorescence imaging, Chem. Soc. Rev. 42 (2013) 622–661.
[7] F. Yu, X. Han, L. Chen, Fluorescent probes for hydrogen sulfide detection and bioimaging, Chem. Commun. 50 (2014) 12234–12249.
[8] S.J. Klebanoff, Myeloperoxidase: friend and foe, J. Leukoc. Biol. Suppl. 77 (2005) 598–625.
[9] S. Fu, M.J. Davies, R. Stocker, R.T. Dean, Evidence for roles of radicals in protein oxidation in advanced human atherosclerotic plaque, Biochem. J. 333 (1998) 519–525.
[10] A.K. Yadav, A. Bracher, S.F. Doran, M. Leustik, G.L. Squadrito, E.M. Postlethwait, S. Matalon, Mechanisms and modification of chlorine-induced lung injury in animals, Proc. Am. Thorac. Soc. 7 (2010) 278–283.
[11] L. Yuan, W. Lin, Y. Xie, B. Chen, J. Song, Fluorescent detection of hypochlorous acid from turn-on to FRET-based ratiometry by a HOCl-mediated cyclization reaction, Chem. Eur. J. 18 (2012) 2700–2706.
[12] Z. Sun, F. Liu, Y, P, K.H. Tam, D. Yang, A highly specific BODIPY-based fluorescent probe for the detection of hypochlorous acid, Org. Lett. 10 (2008) 2171–2174.
[13] J.-J.- Hu, N.K. Wong, Q. Gu, X. Bai, S. Ye, D. Yang, HKOCl-2 series of green BODIPY-based fluorescent probes for hypochlorous acid detection and imaging in live cells, Org. Lett. 16 (2014) 3544–3547.
[14] M. Emrullahoglu, M. Uçuncu, E. Karakus, A BODIPY aldoxime-based chemodosimeter for highly selective and rapid detection of hypochlorous acid, Chem. Commun. 49 (2013) 7836–7838.
[15] H. Zhu, J. Fan, J. Wang, H. Mu, X. Peng, An "Enhanced PET"-based fluorescent probe with ultrasensitivity for imaging basal and elesclomol-induced HClO in cancer cells, J. Am. Chem. Soc. 136 (2014) 12820–12823.
[16] G. Li, D. Zhu, Q. Liu, L. Xue, H. Jiang, A strategy for highly selective detection and imaging of hypochlorite using selenoxide elimination, Org. Lett. 15 (2013) 2002–2005.
[17] Z. Qu, J. Ding, M. Zhao, P. Li, Development of a selenide-based fluorescent probe for imaging hypochlorous acid in lysosomes, J. Photochem. Photobiol. A: Chem. 299 (2015) 1–8.
[18] S.Liu S. Wu, Hypochlorous acid turn-on fluorescent probe based on oxidation of diphenyl selenide, Org. Lett. 15 (2013) 878–881.
[19] L. Yuan, L. Wang, B.-K. Agrawalla, S. Park, H. Zhu, B. Sivaraman, J. Peng, Q. Xu, Y. Chang, Development of targetable two-photon fluorescent probes to image hypochlorous acid in mitochondria and lysosome in live cell and inflamed mouse model, J. Am. Chem. Soc. 137 (2015) 5930–5938.
[20] Y. Jiang, G. Zheng, N. Cai, H. Zhang, Y. Tan, M. Huang, Y. He, J. He, H. Sun, A fast-response fluorescent probe for hypochlorous acid detection and its application in

exogenous and endogenous HOCl imaging of living cells, Chem. Commun. 53 (2017) 12349–12352.
[21] Q. Xu, C.-H. Heo, G. Kim, H.-W. Lee, H.-M. Kim, J. Yoon, Development of imidazoline-2-thiones based two-photon fluorescence probes for imaging hypochlorite generation in a co-culture system, Angew. Chem. Int. Ed. 54 (2015) 4890–4894.
[22] D. Li, Y. Feng, J. Lin, M. Chen, S. Wang, X. Wang, H. Sheng, Z. Shao, M. Zhu, X. Meng, A mitochondria-targeted two-photon fluorescent probe for highly selective and rapid detection of hypochlorite and its bio-imaging in living cells, Sens. Actuators B Chem. 222 (2016) 483–491.
[23] S. Liu, D. Yang, Y. Liu, H. Pan, H. Chen, X. Qu, H. Li, A dual-channel and fast-response fluorescent probe for selective detection of HClO and its applications in live cells, Sens. Actuators B Chem. 299 (2019), https://doi.org/10.1016/j.snb.2019.126937.
[24] B. Zhu, P. Li, W. Shu, X. Wang, C. Liu, Y. Wang, B. Tang, Highly specific and ultrasensitive two-photon fluorescence imaging of native HOCl in lysosomes and tissues based on thiocarbamate derivatives, Anal. Chem. 8824 (2016) 12532–12538.
[25] F. Ali, S. Aute, S. Sreedharan, H.-A. Anila, H.-K. Saeed, C.-G. Smythe, J.-A. Thomas, A. Das, Tracking HOCl concentrations across cellular organelles in real time using a super resolution microscopy probe, Chem. Commun. 54 (2018) 1849–1852.
[26] P. Wei, W. Yuan, F. Xue, W. Zhou, R. Li, D. Zhang, T. Yi, Deformylation reaction-based probe for in vivo imaging of HOCl, Chem. Sci. 9 (2018) 495–501.
[27] B. Zhu, L. Wu, M. Zhang, Y. Wang, Z. Zhao, Z. Wang, Q. Duan, P. Jia, C. Liu, A fast-response, highly specific fluorescent probe for the detection of picomolar hypochlorous acid and its bioimaging applications, Sens. Actuators B Chem. 263 (2018) 103–108.
[28] B. Deng, M. Ren, X. Kong, K. Zhou, W. Lin, Development of an enhanced turn-on fluorescent HOCl probe with a large Stokes shift and its use for imaging HOCl in cells and zebrafish, Sens. Actuators B Chem. 255 (2018) 963–969.
[29] S. Shen, J. Ning, X. Zhang, J. Miao, B. Zhao, Through-bond energy transfer-based ratiometric fluorescent probe for the imaging of HOCl in living cells, Sens. Actuators B Chem. 244 (2018) 907–913.
[30] C. Duan, M. Won, P. Verwilst, J. Xu, H.-S.- Kim, L. Zeng, J.-S.- Kim, In vivo imaging of endogenously produced HClO in zebrafish and mice using a bright, photostable ratiometric fluorescent probe, Anal. Chem. 91 (2019) 4172–4178.
[31] Z. Mao, M. Ye, W. Hu, X. Ye, Y. Wang, H. Zhang, C. Li, Z. Liu, Design of a ratiometric two-photon probe for imaging of hypochlorous acid (HClO) in wounded tissues, Chem. Sci. 9 (2018) 6035–6040.
[32] C. Zhang, Q. Nie, I. Ismail, Z. Xi, L. Yi, A highly sensitive and selective fluorescent probe for fast sensing of endogenous HClO in living cells, Chem. Commun. 54 (2018) 3835–3838.
[33] K. Dou, G. Chen, F. Yu, Z. Sun, G. Li, X. Zhao, L. Chen, J. You, A two-photon ratiometric fluorescent probe for the synergistic detection of the mitochondrial SO_2/HClO crosstalk in cells and in vivo, J. Mater. Chem. B Mater. Biol. Med. 5 (2018) 8389–8398.
[34] S. Kenmoku, Y. Urano, H. Kojima, T. Nagano, Development of a highly specific rhodamine-based fluorescence probe for hypochlorous acid and its application to real-time imaging of phagocytosis, J. Am. Chem. Soc. 129 (2007) 7313–7318.
[35] J. Sun, L. Zhang, Y. Hu, J. Fang, Highly selective fluorometric probes for detection of HClO in living cells, Sens. Actuators B Chem. 266 (2018) 447–454.
[36] H. Zhang, C. Zhang, R. Liu, L. Yi, H. Sun, A highly selective and sensitive fluorescent thiol probe through dual-reactive and dual-quenching groups, Chem. Commun. 51 (2015) 2029–2032.
[37] C. Zhang, L. Wei, C. Wei, J. Zhang, R. Wang, Z. Xi, L. Yi, A FRET-ICT dual-quenching fluorescent probe with large off-on response for H_2S: synthesis, spectra and bioimaging, Chem. Commun. 51 (2015) 7505–7508.
[38] C. Wei, R. Wang, C. Zhang, G. Xu, Y. Li, Q.-Z. Zhang, L.-Y. Li, L. Yi, Z. Xi, Dual-reactable fluorescent probes for highly selective and sensitive detection of biological H_2S, Chem. - Asian J. 11 (2016) 1376–1381.
[39] C. Zhang, R. Wang, L. Cheng, B. Li, Z. Xi, L. Yi, A redox-nucleophilic dual-reactable probe for highly selective and sensitive detection of H_2S: synthesis, spectra and bioimaging, Sci. Rep. 6 (2016) 30148.
[40] X. Song, W. Hu, D. Wang, Z. Mao, Z. Liu, A highly specific and ultrasensitive probe for the imaging of inflammation-induced endogenous hypochlorous acid, Analyst 144 (2019) 3546–3551.
[41] X. Liu, M. Xiang, Z. Tong, F. Luo, W. Chen, F. Liu, F. Wang, R.-Q. Yu, Activatable fluorescence probe via self-immolative intramolecular cyclization for histone deacetylase imaging in live cells and tissues, Anal. Chem. 90 (2018) 5534–5539.
[42] Y. Jung, I.G. Ju, Y.H. Choe, Y. Kim, S. Park, Y.-M. Hyun, M.S. Oh, Hydrazine expose: the next-generation fluorescent probe, ACS Sensor. 4 (2019) 441–449.
[43] A.S. Rao, D. Kim, T. Wang, K.H. Kim, S. Hwang, K.H. Ahn, Reaction-based two-photon probes for mercury Ions: fluorescence imaging with dual optical windows, Org. Lett. 14 (2012) 2598–2601.
[44] A.E. Albers, V.S. Okreglak, C.J. Chang, A FRET-based approach to ratiometric fluorescence detection of hydrogen peroxide, J. Am. Chem. Soc. 128 (2006) 9640–9641.
[45] L. Wu, Y. Wang, M. Weber, L. Liu, A.C. Sedgwick, S.D. Bull, C. Huang, T.D. James, ESIPT-based ratiometric fluorescence probe for the intracellular imaging of peroxynitrite, Chem. Commun. 54 (2018) 9953–9956.
[46] Y. Wu, A. Shi, Y. Li, H. Zeng, X. Chen, J. Wu, X. Fan, A near-infrared xanthene fluorescence probe for monitoring peroxynitrite in living cells and mouse inflammation model, Analyst 143 (2018) 5512–5519.
[47] M. Abo, Y. Urano, K. Hanaoka, T. Terai, T. Komatsu, T. Nagano, Development of a highly sensitive fluorescence probe for hydrogen peroxide, J. Am. Chem. Soc. 133 (2011) 10629–10637.
[48] Y. Jiang, G. Zheng, Q. Duan, L. Yang, J. Zhang, H. Zhang, J. He, H. Sun, D. Ho, Ultra-sensitive fluorescent probes for hypochlorite acid detection and exogenous/endogenous imaging of living cells, Chem. Commun. 54 (2018) 7967–7970.
[49] E.K.U. Gross, W. Kohn, Local density-functional theory of frequency-dependent linear response, Phys. Rev. Lett. 55 (1985) 2850–2852.
[50] R.E. Stratmann, G.E. Scuseria, M.J. Frisch, An efficient implementation of time-dependent density-functional theory for the calculation of excitation energies of large molecules, J. Chem. Phys. 109 (1998) 8218–8224.
[51] Y. Zhang, K. Wang, G. Zhuang, Z. Xie, C. Zhang, F. Cao, G. Pan, H. Chen, B. Zou, Y. Ma, Multicolored-fluorescence switching of ICT-type organic solids with clear color difference: mechanically controlled excited state, Chem.- Euro. J. 21 (2015) 2474–2479.
[52] S. Arimori, L.I. Bosch, C.J. Ward, T.D. James, Fluorescent internal charge transfer (ICT) saccharide sensor, Tetrahedron Lett. 42 (2001) 4553–4555.
[53] F. Tian, Y. Jia, Y. Zhang, W. Song, G. Zhao, Z. Qu, C. Li, Y. Chen, P.LI A HClO-specific near-infrared fluorescent probe for determination of Myeloperoxidase activity and imaging mitochondrial HClO in living cells, Biosens. Bioelectron. 86 (2016) 68–74.
[54] T. Peng, N.-K. Wong, X. Chen, Y.-K. Chan, D.H.-H. Ho, Z. Sun, J.J. Hu, J. Shen, H. Elnezami, D. Yang, Molecular imaging of peroxynitrite with HKGreen-4 in live cells and tissues, J. Am. Chem. Soc. 136 (2014) 11728–11734.
[55] X. Li, R.-R. Tao, L.-J. Hong, J. Cheng, Q. Jiang, Y.-M. Lu, M.-H. Liao, W.-F. Ye, N.-N. Lu, F. Han, Y.-Z. Hu, Y.-H. Hu, Visualizing peroxynitrite fluxes in endothelial cells reveals the dynamic progression of brain vascular injury, J. Am. Chem. Soc. 137 (2015) 12296–12303.
[56] J.J. Hu, N.-K. Wong, M.-Y. Lu, X. Chen, S. Ye, A.Q. Zhao, P. Gao, R.Y.-T. Kao, J. Shen, D. Yang, HKOCl-3: a fluorescent hypochlorous acid probe for live-cell and in vivo imaging and quantitative application in flow cytometry and a 96-well microplate assay, Chem. Sci. 7 (2016) 2094–2099.
[57] H. Zhang, R. Liu, Y. Tan, W.H. Xie, H. Lei, H.Y. Cheung, H. Sun, A FRET-based ratiometric fluorescent probe for nitroxyl detection in living cells, ACS Appl. Mater. Inter. 7 (2015) 5438–5443.
[58] H. Zhang, L. Feng, Y. Jiang, Y.-T. Wong, Y. He, G. Zheng, J. He, Y. Tan, H. Sun, D. Ho, A reaction-based near-infrared fluorescent sensor for Cu^{2+} detection in aqueous buffer and its application in living cells and tissues imaging, Biosens. Bioelectron. 94 (2017) 24–29.
[59] C.S. Lim, G. Masanta, H.J. Kim, J.H. Han, H.M. Kim, B.R. Cho, Ratiometric detection of mitochondrial thiols with a two-photon fluorescent probe, J. Am. Chem. Soc. 133 (2011) 11132–11135.
[60] H.M. Kim, H.-J. Choo, S.-Y. Jung, Y.-G. Ko, W.-H. Park, S.-J. Jeon, C.H. Kim, T. Joo, B.R. Cho, A two-photon fluorescent probe for lipid raft imaging: C-laurdan, ChemBioChem 8 (2007) 553–559.
[61] P. Zhang, H. Wang, Y. Hong, M. Yu, R. Zeng, Y. Long, J. Chen, Selective visualization of endogenous hypochlorous acid in zebrafish during lipopolysaccharide-induced acute liver injury using a polymer micelles-based ratiometric fluorescent probe, Biosens. Bioelectron. 99 (2018) 318–324.
[62] S.-L. Shen, X.-F. Zhang, Y.-Q. Ge, Y. Zhu, X.-Q. Cao, A novel ratiometric fluorescent probe for the detection of HOCl based on FRET strategy, Sens. Actuators B Chem. 254 (2018) 736–741.
[63] P. Arvadia, M. Narwaley, R.M. Whittal, A.G. Siraki, 4-Aminobenzoic acid hydrazide inhibition of microperoxidase-11: catalytic inhibition by reactive metabolites, Arch. Biochem. Biophys. 515 (2011) 120–126.
[64] A.J. Kettle, C.A. Gedye, C.C. Winterbourn, Mechanism of inactivation of myeloperoxidase by 4-aminobenzoic acid hydrazide, Biochem. J. 321 (1997) 503–508.
[65] S. Galijasevic, The development of myeloperoxidase inhibitors, Bioorg. Med. Chem. Lett. 29 (2019) 1–7.
[66] L. Li, C.-W. Zhang, G.Y.J. Chen, B. Zhu, C. Chai, Q.-H. Xu, E.-K. Tan, Q. Zhu, K.-L. Lim, S.Q. Yao, A sensitive two-photon probe to selectively detect monoamine oxidase B activity in Parkinson's disease models, Nat. Commun. 5 (2014) 3276.
[67] H. Zhang, P. Xiao, Y.T. Wong, W. Shen, M. Chhabra, R. Peltier, Y. Jiang, Y. He, J. He, Y. Tan, Y. Xie, D. Ho, Y.-W. Lam, J. Sun, H. Sun, Construction of an alkaline phosphatase-specific two-photon probe and its imaging application in living cells and tissues, Biomaterials 140 (2017) 220–229.
[68] Y. Feng, S. Li, D. Li, Q. Wang, P. Ning, M. Chen, X. Tian, X. Wang, Rational design of a diaminomaleonitrile-based mitochondria-targeted two-photon fluorescent probe for hypochlorite in vivo: solvent-independent and high selectivity over Cu^{2+}, Sens. Actuators B Chem. 254 (2018) 282–290.
[69] D. Li, Y. Feng, J. Lin, M. Chen, S. Wang, X. Wang, H. Sheng, Z. Shao, M. Zhu, X. Meng, A mitochondria-targeted two-photon fluorescent probe for highly selective and rapid detection of hypochlorite and its bio-imaging in living cells, Sens. Actuators B Chem. 222 (2016) 483–491.
[70] P. Ning, W. Wang, M. Chen, Y. Feng, X. Meng, Recent advances in mitochondria- and lysosomes-targeted small-molecule two-photon fluorescent probes, Chin. Chem. Lett. 28 (2017) 1943–1951.
[71] C. Xu, W.W. Webb, Measurement of two-photon excitation cross sections of molecular fluorophores with data from 690 to 1050 nm, J. Opt. Soc. Am. B 13 (1996) 481–491.
[72] M.A. Albota, C. Xu, W.W. Webb, Two-photon fluorescence excitation cross sections of biomolecular probes from 690 to 960 nm, Pure Appl. Opt. J. Eur. Opt. Soc. Part A 37 (1998) 7352–7356.
[73] E. Malle, T. Buch, H.J. Grone, Myeloperoxidase in kidney disease, Kidney Int. 64 (2003) 1956–1967.
[74] E. Malle, C. Woenckhaus, G. Waeg, H. Esterbauer, E.F. Groene, H.-J. Groene, Immunological evidence for hypochlorite-modified proteins in human kidney, Am. J. Pathol. 150 (1997) 603–615.

Guansheng Zheng received his master degree from Guangdong University of

Technology, and he is a research assistant in City University of Hongkong under the direction of Prof. Hongyan Sun now.

Zejun Li is studying for her master degree in Guangdong University of Technology.

Qinya Duan is studying for her master degree in Guangdong University of Technology.

Ke Cheng received his master degree from Jinan University in 2018. He is currently a PhD student in City University of HongKong and major in fluorescent probes.

Yong He is studying for her master degree in Guangdong University of Technology.

Shumei Huang is studying for her master degree in Guangdong University of Technology.

Huatang Zhang received his PhD in Chemistry from City University of HongKong in 2015. He is working as an associate professor in Guangdong University of Technology. His research interests focus on development of organic and inorganic fluorescent sensors for bioimaging and drug release.

Yin Jiang received her PhD degree from Lanzhou University in 2014. She is an associate professor in Guangdong University of Technology now. Her research interests focus on design and synthesis of biosensors for real-time bioimaging detection.

Yongguang Jia received his PhD degree from Nankai University in 2012. He is an associate professor in South China University of Technology now.

Hongyan Sun is currently an associate professor in City University of HongKong and core member of Centre of Super-Diamond and Advanced Films. She has published more than one-hundred research articles. Her current interests are bioorganic chemistry, microarray, cell-based assay, biosensors and biomaterials